



## Breakable Hybrid Organosilica Nanocapsules for Protein Delivery

Eko Adi Prasetyanto,\* Alessandro Bertucci, Dedy Septiadi, Roberto Corradini, Pablo Castro-Hartmann, and Luisa De Cola\*

**Abstract:** The direct delivery of specific proteins to live cells promises a tremendous impact for biological and medical applications, from therapeutics to genetic engineering. However, the process mostly involves tedious techniques and often requires extensive alteration of the protein itself. Herein we report a straightforward approach to encapsulate native proteins by using breakable organosilica matrices that disintegrate upon exposure to a chemical stimulus. The biomolecule-containing capsules were tested for the intracellular delivery of highly cytotoxic proteins into C6 glioma cells. We demonstrate that the shell is broken, the release of the active proteins occurs, and therefore our hybrid architecture is a promising strategy to deliver fragile biomacromolecules into living organisms.

Intracellular delivery of particular proteins holds an important role in biology and medicine, from restoring the function of interest, producing highly specific molecules in situ, to regulating gene expression without any genomic alteration that leads to a reprogramming of the cell behavior.<sup>[1]</sup> Innovations in biotechnology and nanomedicine have led to a significant increase in the number of protein- and peptide-based therapeutics and other macromolecular drugs. Furthermore, recent advances in genomic and proteomic technologies are expected to continue to expand the pipeline of molecular curative candidates.<sup>[2]</sup> Nevertheless, the efficient delivery of native, functional proteins or enzymes, in an active conformation to the necessary site of action, still remains a challenge. Under physiological conditions, proteins and peptides tend to undergo degradation by proteolytic enzymes or, in the case of the higher-molecular-weight proteins, may be recognized by neutralizing antibodies.<sup>[3]</sup> To overcome these limitations, proper delivery systems must be able to shield and to protect the bioactive molecules in order to preserve their

functional nature, reducing the need for repetitive injections, and without compromising the biological activity of the protein.<sup>[4]</sup>

Protein stabilization for delivery purposes has mainly been achieved by micro- and nano-encapsulation (e.g., within liposomes, polymeric, or inorganic structures)<sup>[5]</sup> and bioconjugation (i.e., covalently linking proteins with water-soluble polymers or simply crosslinking proteins to form stable particle complexes).<sup>[1a,6]</sup> In vitro protein delivery has been addressed by using protein-coated gold-nanoparticle-stabilized nanocapsules, however the proteins were still exposed to the surrounding environment.<sup>[7]</sup> Encapsulation strategies have received more and more attention and some examples of diverse soft host structures have been reported.<sup>[8]</sup> Mostly polymeric assemblies having biodegradable or, even better, stimuli-responsive networks for controlled release have been described.<sup>[9]</sup> However this encapsulation strategy may suffer from a lack of stability since only physical interactions occur between the polymer framework and the protein cargo.<sup>[10]</sup>

Very recently Tasciotti et al. reported silicon degradable nanoneedles for delivering RNA.<sup>[11]</sup> Furthermore, the use of porous or hollow silica has emerged as one of the most promising strategies in the field of nanomedicine.<sup>[12]</sup> However, to the best of our knowledge, no examples of biodegradable hybrid silica shells for the encapsulation and subsequent release of large biomolecules have been reported. Herein we describe the development of an innovative system able to encapsulate functional proteins in their active folding. The capsules possess excellent stability in water, and are engineered to break into very small pieces (< 5 nm) once internalized into cells. The natural reducing environment of the cells is used to trigger the disruption of the shell.

We demonstrate that the construction of the breakable shell around the proteins is a general methodology and different bioactive macromolecules can be entrapped and released from the stimulus-responsive container. As a model protein we used cytochrome C (CyC), as its strong absorption in the visible region allows us to study the kinetics of release by UV/Vis absorption spectroscopy. We then extended the investigation to other proteins known to be effective for killing cancer cells, such as the cytotoxic TRAIL Apo2 ligand and onconase.<sup>[13]</sup> The capsules containing any of the toxic proteins were tested in vitro as a possible treatment towards glioblastoma, one of the most aggressive cancers with a survival rate as low as five years.<sup>[14]</sup>

The first proof of the successful encapsulation is given by the formation of nanoparticles and their UV/Vis absorption profile. The realization of the shell, in order to prevent denaturation of the biomolecule, was performed following the reverse nanoemulsion procedure described in the experimental section (see Figure 1 for a general description). The silica

[\*] Dr. E. A. Prasetyanto, Dr. A. Bertucci, Dr. D. Septiadi, Prof. L. De Cola  
Institut de science et d'ingénierie supramoléculaires (ISIS)  
Université de Strasbourg  
8 Allée Gaspard Monge, 67083 Strasbourg (France)  
E-mail: prasetyanto@unistra.fr  
decola@unistra.fr

Dr. A. Bertucci, Prof. R. Corradini  
Dipartimento di Chimica, Università di Parma  
Parma (Italy)

Dr. P. Castro-Hartmann  
Servei de Microscòpia, Universitat Autònoma de Barcelona  
Bellaterra (Spain)

Prof. L. De Cola  
Institute of Nano Technology (INT)  
Karlsruhe Institute of Technology, Karlsruhe (Germany)

Supporting information and ORCID(S) from the author(s) for this article are available on the WWW under <http://dx.doi.org/10.1002/anie.201508288>.

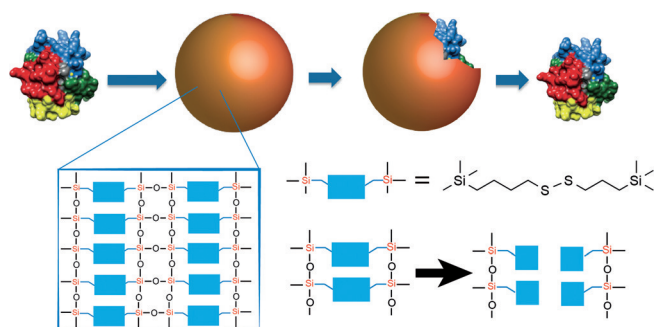


**Figure 1.** Construction of the breakable silica capsules. The protein cargo is encapsulated within a breakable hybrid shell that comprises disulfide bridges embedded in a silica network.

network of the formed capsules contains about 30 % of organic material made of the bispropyldisulfide (see Figure 1) derivatives, representing the redox-sensitive groups. Well-defined nanospheres, uniform in size, possessing a diameter around 40–50 nm were obtained (CyC@BS-NP), as shown in the SEM pictures (Figure 2A). A similar size (65 nm) was measured by dynamic light scattering measurements on a suspension of the capsules in water. Interestingly, the materials remain intact even after 10 months storage of the solution at 4 °C and the dispersion and size confirm no aggregation or destruction of the capsules (see Figure S1A and S1B in the Supporting Information). The morphology, shape, and size of the obtained capsules have been analyzed in more detail by HR-TEM measurements (Figure 2B and Figure S1B). The material was suspended in a sodium borohydride solution (see the Supporting Information for details) and cryo-TEM images were taken after 1 h and 3 h exposure to the reducing agent, (Figure 2C,D) to monitor the destruction of the capsules through the reduction of the disulfide groups. In an analogous manner we have prepared and analyzed nonbreakable particles that lack the S–S moieties, but contain the same protein. They show very similar size and morphology (Figure S2 in the Supporting Information) but do not display any degradation in the same reducing agent solution.

To evaluate the release kinetics of cytochrome C from the breakable nanocapsules, upon their destruction, the particles were dispersed in water and incubated with glutathione (5 mM; mimicking a concentration present in living cells). Analysis of the supernatant with UV/Vis spectroscopy revealed the absorption of the cytochrome C released from the destroyed particles. The results summarized in Figure 2E show that at time = 0 (before adding glutathione) there is no signal of the protein in solution. Upon addition of glutathione, already after 1 hour, a detectable absorption appeared at around 400 nm. The signal then increased over time, as the cytochrome C left the broken capsules and dissolved into water. After 24 h, the signal reached a plateau, thus suggesting that almost the overall protein escape took place in one day (Figure S3). Analysis of the supernatant by mass spectrometry also confirms the presence of CyC in solution (Figure S4). As a control experiment we have compared the release from the nonbreakable capsules, using the same

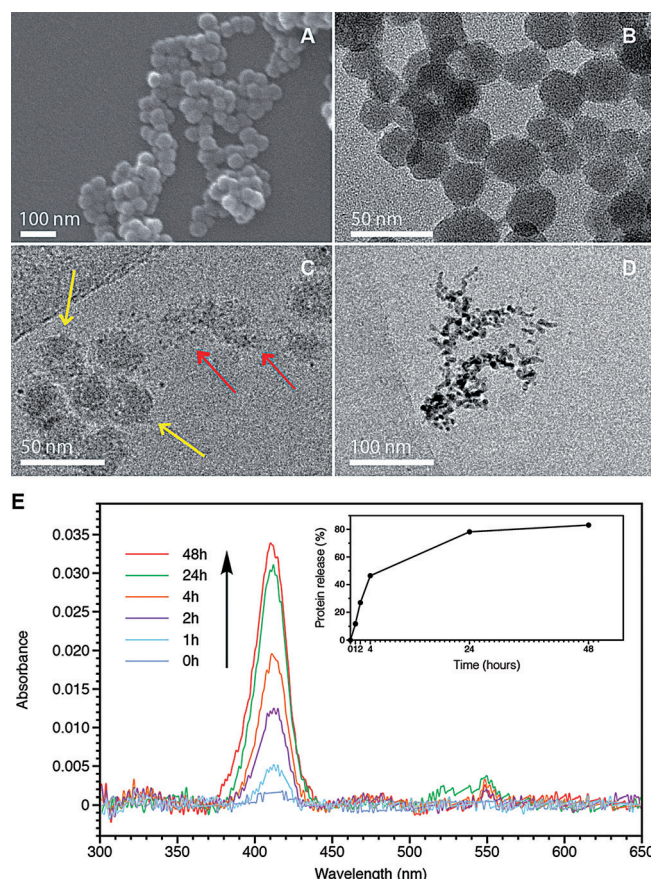


**Figure 2.** Characterization of the material and release kinetics. A) SEM image of synthesized CyC@BS-NPs, B) HR-TEM images of intact CyC@BS-NPs, and C, D) cryo-TEM images of the same particles after treatment with a solution of NaBH<sub>4</sub> for 1 h and 3 h, respectively. E) UV/Vis spectra of the supernatants recovered after treating CyC@BS-NPs with glutathione, in aqueous solution. The signal monitored is due to the main electronic transitions of the released cytochrome C. Inset: release profile over time at fixed wavelength ( $\lambda_{\text{abs}} = 410 \text{ nm}$ ).

amount of cytochrome C (CyC@NonBS-NPs), and observed no protein in solution even after 48 h (Figure S5). From the absorption feature we have also calculated the number of proteins per particle (about 31), and their almost quantitative (> 90 %) release from the broken capsules (see the Supporting Information for more data).

To exploit the use of these carriers in living cells, and therefore their possible applications for protein delivery, we performed cellular uptake experiments by incubating CyC@NPs on living C6 glioma cells. The internalization of the materials, was followed by SEM (Figure S6). The cells rapidly internalized small numbers of particles only 7 min after starting the incubation, and the amount of material taken up increased over time (Figure S6C,D). Since SEM can only visualize what is happening on the cell surface, we performed further studies by using TEM on the cells after they were incubated with the particles. The aim of this experiment is also to observe the effect of the reducing agent (glutathione present in the biological environment) on the



breakable shell. We also compared the different response between the investigated system, CyC@BS-NPs, and the nonbreakable shells (see Figure 3A for a pictorial description). The experiments were carried out by analyzing the internalized particles at different incubation times that is, 4 and 24 h (Figure 3B,C,D) at a concentration of particles of  $0.1 \text{ mg mL}^{-1}$ .

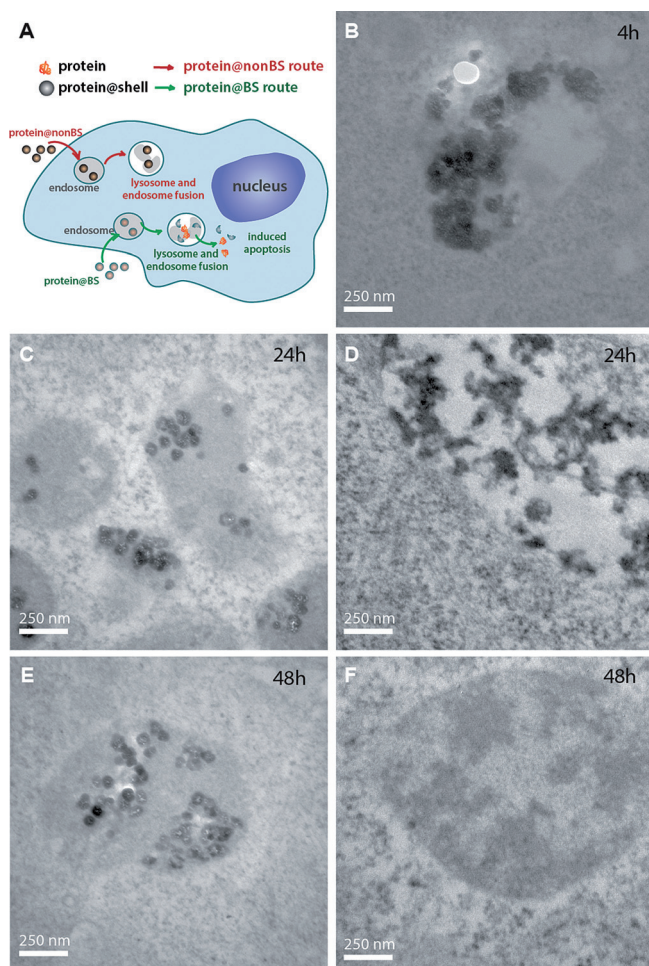


**Figure 3.** Transmission electron micrographs of internalized particles in cells. C6 glioma cells were incubated for 4 and 24 h with  $0.1 \text{ mg mL}^{-1}$  particle dispersion (CyC@BS-NPs and CyC@NonBS-NPs respectively) and cultured for additional 24 h after changing the culture media. Panel A shows a schematic representation of the nanoparticle internalization and their fate in the cell. Images B, D, F: breakable particles. Images C and E: nonbreakable nanomaterials.

One experiment was prolonged to 48 h: the cells were incubated with the nanoparticles for 24 h and, after washing away the particles, a further 24 h incubation was performed in clean cell culture media (48 h in Figure 3E and F).

TEM images clearly indicate that the nanomaterials are compartmentalized and after 4 h even the breakable particles are still mostly intact. Interestingly, after 24 h, the breaking of the particles, triggered by the lysosomal enzymatic activity,

occurs and only a multitude of amorphous morphologies are detectable (Figure 3D). The destruction of the organosilica shell is complete after 48 h, and aggregated debris, which give a diffuse contrast to the lysosome, are observed (Figure 3F). The nonbreakable particles do not show any degradation even after 48 h incubation, and maintain the typical round shape (Figure 3C and E) of the freshly synthesized particles (Figure 2B).

In order to visualize and colocalize the particles, we encapsulated a green fluorescent protein, EGFP, in the breakable capsules, as probe for confocal microscopy, and also to prove that the encapsulation can occur with different type of proteins (Figure S7). Incubation of the EGFP@BS-NP with C6 glioma cells (see Figure 4A,B), showed colocalization into the lysosome and the degradation results are in accordance with the breaking behavior observed by TEM for the CyC@BS-NP. In this case, the release of EGFP into the cytoplasm results in a diffused non-colocalized emission signal because of the spreading of the fluorescent proteins into the cytoplasm (see Figure S8 and S9).

Finally, to demonstrate that the shell is protecting and maintaining the activity of the intact macromolecules, we next encapsulated toxic proteins such as human TRAIL Apo2 ligand (TRAIL@BS-NP) and onconase (oncon@BS-NP) in breakable shell nanocapsules (Figure S4).

TRAIL Apo2 ligand is a protein that belongs to the tumor necrosis factor (TNF) family of death ligands and can be used to overcome resistance to conventional chemotherapeutic drugs. TRAIL@BS-NPs were thus initially tested on a C6 glioma cell line, and toxicity can be expected only when the protein is delivered into the cytosol in its native folding. To have a full quantification of the toxicity of the material, we also investigated the same type and number of cells after incubation with the potentially nontoxic CyC@BS-NP and CyC@NonBS-NPs.

The overall cell viability was measured as direct indicator of the cytotoxic/anticancer effect provided by the hybrid particles. The results are summarized in the plot in Figure 4C and show that CyC@NonBS-NPs did not influence the total cell viability with respect to the control culture, thus confirming that the core/shell system is absolutely biocompatible and noncytotoxic (Figure 4C). In the case of CyC@BS-NPs, a slight reduction of the viability was recorded (78.7% vs. 89.5% control), which can be possibly ascribed to an interference effect in the normal biological metabolism because of an excess of cytochrome C present in the cell after the delivery, thus inducing apoptosis.<sup>[15]</sup>

An important result, shown in Figure 4C, is the cell viability percentage obtained when treating the C6 glioma cells with TRAIL@BS-NP ( $0.15 \text{ mg mL}^{-1}$ , 24 h), which induced a drastic reduction of the value up to 45% with respect to the control sample. The results highlight the effective role of the nanosphere system internalized by the cell: the ability to deliver the protein in the native form upon degradation of the outer shell. The released TRAIL must be in an active conformation to carry on its apoptosis-inducing effect, as indicated by the overall cell viability reduction. To confirm this effect, the same TRAIL@BS-NPs were also used to incubate C6 glioma cells under the same conditions, which

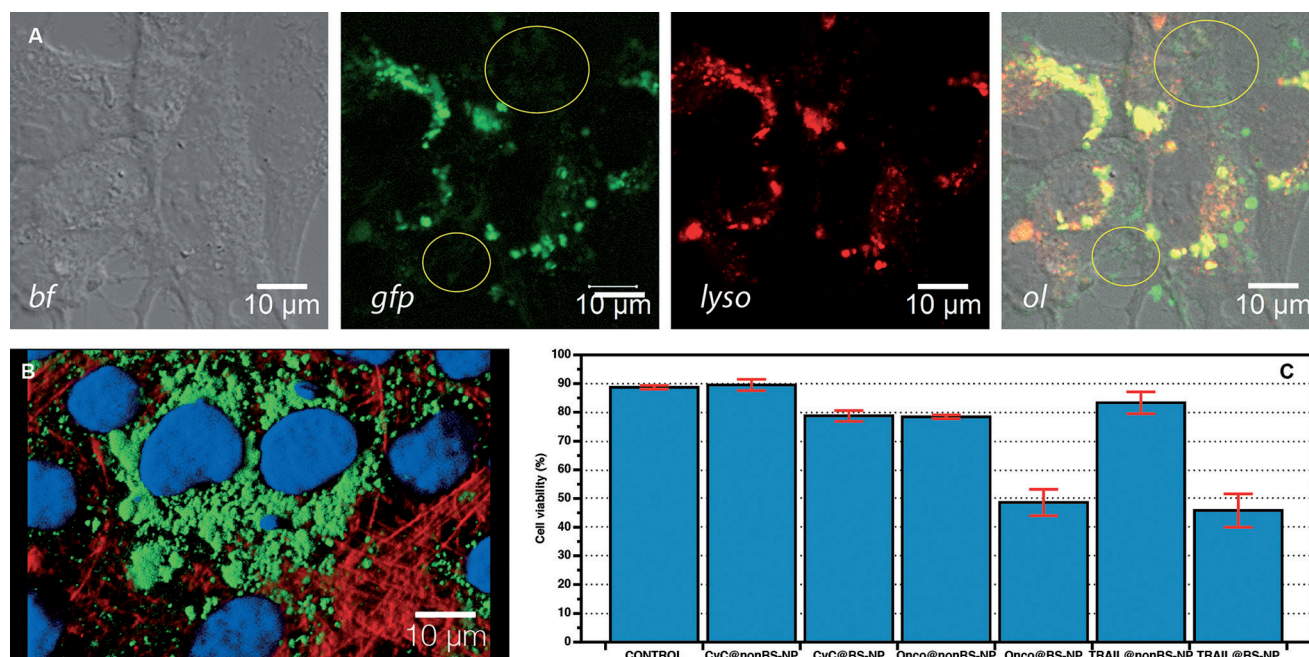


**Figure 4.** A) Confocal micrographs taken after 24 h incubation with the particles (concentration  $0.05 \text{ mg mL}^{-1}$ ) showing the localization of the particles in C6 glioma cells. Colocalization experiments with LysoTracker® Red DND-99 revealed the sublocalization of particles in lysosome area (overlap coefficient 0.87). Green color: signal from EGFP, red corresponds to lysosome. Yellow circle: non-colocalized area of released EGFP with lysosome. Scale bars =  $10 \mu\text{m}$ . B) Top view of 3D confocal microscopy image of f-actin (red) and nucleus-stained (blue) C6 cells taking up EGFP-containing particles (green). Excitation wavelengths are 405, 488, 594, and 633 nm for DAPI, EGFP, LysoTracker Red DND-99, and Alexa Fluor 647 Phalloidin, respectively. C) Summary of cell viability tests.

were eventually analyzed in a Trypan Blue cell mortality test (Figure S10).

The role played by the breakable disulfide-containing shell and its potential as chemotherapeutic tool was corroborated when viability experiments were conducted on the same cell line using Onco@BS-NP and compared with the non-breakable nanoparticles, Onco@NonBS-NP. The nanomaterials were synthesized and incubated with C6 glioma. The cytotoxicity experiments were then performed as outlined above, and once again the cell viability was employed to evaluate the integrity of the protein and its activity as cell inducing apoptosis. It is important to note that Onco@NonBS-NP did not affect the cell viability, as no significant change could be registered with respect to the control sample (Figure 4C). The excellent biocompatibility of the material is also an indicator that the protein cargo cannot leak out when the nanocapsule shell is made entirely of silica, and the selected proteins are not present on the silica surface. On the other hand, when treating the cells with Onco@BS-NP ( $0.15 \text{ mg mL}^{-1}$ , 24 h), a dramatic drop (up to 40%) of the viability percentage was observed. This result demonstrates that the delivery of onconase occurs upon degradation of the breakable shell. The data strongly suggest that the onconase was thus released in its functional conformation, able to carry on its related antitumor effect (for a summary of the data see Table 1 in the Supporting Information).

In conclusion, we have proposed a general method for the encapsulation of proteins within a stimulus-responsive breakable hybrid organosilica shell. The breaking of the capsules is

efficient once the nanocapsules are internalized in cancer cells and the released proteins retained their activity.

### Experimental Section

**Synthesis of CyC@BS-NP:** Triton X-100 (1.77 mL) and *n*-hexanol (1.8 mL) were dissolved in cyclohexane (7.5 mL). Separately, 300  $\mu\text{L}$  of a  $2.5 \text{ mg mL}^{-1}$  aqueous solution of cytochrome C from equine heart were mixed with 40  $\mu\text{L}$  of tetraethyl orthosilicate (TEOS) and 60  $\mu\text{L}$  of bis[3-(triethoxysilyl)propyl]disulfide. After shaking, this mixture was added to the organic solution. 50  $\mu\text{L}$  of 30% aqueous ammonia solution was added and the water–oil emulsion was stirred overnight at room temperature. 20 mL of pure acetone was subsequently added in order to precipitate the CyC@BS-NPs and the material was recovered by centrifugation, washing twice with ethanol, and three times with water. Encapsulation of other protein and cell experiment is described in the Supporting Information.

### Acknowledgements

E.A.P., D.S., and L.D.C. acknowledge financial support from the European Research Council for the ERC Advanced Grant (Grant Agreement no. 2009-247365) and Fondation ARC project “Thera-HCC” grant IHU201301187. A.B. and R.C. thank the French Embassy in Italy and the French government for providing the MAEE grant for scientific cooperation between Italy and France (number 778588G). We thank to Dr. Eita Sasaki and Prof. Donald Hilvert for providing the onconase protein.



**Keywords:** encapsulation · hybrid materials · nanostructures · organosilica · protein delivery

**How to cite:** *Angew. Chem. Int. Ed.* **2016**, *55*, 3323–3327  
*Angew. Chem.* **2016**, *128*, 3384–3388

- [1] a) J. Jo, S. Hong, W. Y. Choi, D. R. Lee, *Sci. Rep.* **2014**, *4*, 1–8; b) H. Zhou, S. Wu, J. Y. Joo, S. Zhu, D. W. Han, T. Lin, S. Trauger, G. Bien, S. Yao, Y. Zhu, G. Siuzdak, H. R. Schöler, L. Duan, S. Ding, *Cell Stem Cell* **2009**, *4*, 381–384; c) S. R. Schwarze, A. Ho, A. Vocero-Akbani, S. F. Dowdy, *Science* **1999**, *285*, 1569–1572.
- [2] a) T. C. G. A. Network, *Nature* **2012**, *490*, 61–70; b) A. M. Shah, D. L. Mann, *Lancet* **2011**, *378*, 704–712; c) M. Tyers, M. Mann, *Nature* **2003**, *422*, 193–197.
- [3] a) K. Fu, A. M. Klibanov, R. Langer, *Nat. Biotechnol.* **2000**, *18*, 24–25; b) W. Jiskoot, T. W. Randolph, D. B. Volkin, C. R. Middaugh, C. Schöneich, G. Winter, W. Friess, D. J. A. Crommelin, J. F. Carpenter, *J. Pharm. Sci.* **2012**, *101*, 946–954.
- [4] a) Z. Gu, A. Biswas, M. Zhao, Y. Tang, *Chem. Soc. Rev.* **2011**, *40*, 3638–3655; b) J. Du, J. Jin, M. Yan, Y. Lu, *Curr. Drug Metab.* **2012**, *13*, 82–92.
- [5] a) X. Wu, Y. Song, J. Han, L. Yang, S. Han, *Biomater. Sci.* **2013**, *1*, 918; b) M. Wang, K. Alberti, S. Sun, C. L. Arellano, Q. Xu, *Angew. Chem. Int. Ed.* **2014**, *53*, 2893–2898; *Angew. Chem.* **2014**, *126*, 2937–2942; c) H. Shen, M. Liu, Y. Chong, J. Huang, Z. Zhang, *Toxicol. Res.* **2013**, *2*, 379.
- [6] a) G. Pasut, F. Veronese in *Polymer Therapeutics I*, Vol. 192 (Eds.: R. Satchi-Fainaro, R. Duncan), Springer, Berlin, **2006**, pp. 95–134; b) K. Montrose, Y. Yang, X. Sun, S. Wiles, G. W. Krissansen, *Sci. Rep.* **2013**, *3*, 1661; c) S. B. Fonseca, M. P. Pereira, S. O. Kelley, *Adv. Drug Delivery Rev.* **2009**, *61*, 953–964.
- [7] a) R. Tang, C. S. Kim, D. J. Solfiell, S. Rana, R. Mout, E. M. Velázquez-Delgado, A. Chompoosor, Y. Jeong, B. Yan, Z.-J. Zhu, C. Kim, J. A. Hardy, V. M. Rotello, *ACS Nano* **2013**, *7*, 6667–6673; b) P. Ghosh, X. Yang, R. Arvizo, Z.-J. Zhu, S. S. Agasti, Z. Mo, V. M. Rotello, *J. Am. Chem. Soc.* **2010**, *132*, 2642–2645; c) C. S. Kim, R. Mout, Y. Zhao, Y.-C. Yeh, R. Tang, Y. Jeong, B. Duncan, J. A. Hardy, V. M. Rotello, *Bioconjugate Chem.* **2015**, *26*, 950–954.
- [8] a) E. Yuba, A. Harada, Y. Sakanishi, S. Watarai, K. Kono, *Biomaterials* **2013**, *34*, 3042–3052; b) L. J. White, G. T. S. Kirby, H. C. Cox, R. Qodratnama, O. Qutachi, F. R. A. J. Rose, K. M. Shakesheff, *Mater. Sci. Eng. C* **2013**, *33*, 2578–2583.
- [9] a) M. Zhao, A. Biswas, B. Hu, K.-I. Joo, P. Wang, Z. Gu, Y. Tang, *Biomaterials* **2011**, *32*, 5223–5230; b) T. Akagi, Y. Zhu, F. Shima, M. Akashi, *Biomater. Sci.* **2014**, *2*, 530–537; c) S. Santra, C. Kaittanis, J. M. Perez, *Mol. Pharm.* **2010**, *7*, 1209–1222.
- [10] M. van de Weert, W. Hennink, W. Jiskoot, *Pharm. Res.* **2000**, *17*, 1159–1167.
- [11] C. Chiappini, E. De Rosa, J. O. Martinez, X. Liu, J. Steele, M. M. Stevens, E. Tasciotti, *Nat. Mater.* **2015**, *14*, 532–539.
- [12] a) C. Argyo, V. Weiss, C. Bräuchle, T. Bein, *Chem. Mater.* **2014**, *26*, 435–451; b) D. Wang, Z. Xu, Z. Chen, X. Liu, C. Hou, X. Zhang, H. Zhang, *ACS Appl. Mater. Interfaces* **2014**, *6*, 12600–12608; c) Y. Piao, A. Burns, J. Kim, U. Wiesner, T. Hyeon, *Adv. Funct. Mater.* **2008**, *18*, 3745–3758; d) M. Montalti, L. Prodi, E. Rampazzo, N. Zaccheroni, *Chem. Soc. Rev.* **2014**, *43*, 4243–4268; e) I. I. Slowing, B. G. Trewyn, V. S. Y. Lin, *J. Am. Chem. Soc.* **2007**, *129*, 8845–8849.
- [13] a) K. Shah, Y. Tang, X. Breakefield, R. Weissleder, *Oncogene* **2003**, *22*, 6865–6872; b) W. Ardel, K. Shogen, Z. Darzynkiewicz, *Curr. Pharm. Biotechnol.* **2008**, *9*, 215–225.
- [14] a) R. Stupp, M. E. Hegi, W. P. Mason, M. J. van den Bent, M. J. B. Taphoorn, R. C. Janzer, S. K. Ludwin, A. Allgeier, B. Fisher, K. Belanger, P. Hau, A. A. Brandes, J. Gijtenbeek, C. Marosi, C. J. Vecht, K. Mokhtari, P. Wesseling, S. Villa, E. Eisenhauer, T. Gorlia, M. Weller, D. Lacombe, J. G. Cairncross, R.-O. Mirimanoff, *Lancet Oncol.* **2009**, *10*, 459–466; b) S. Ni, X. Fan, J. Wang, H. Qi, X. Li, *Ann. Biomed. Eng.* **2014**, *42*, 214–221; c) Z. Lwin, D. MacFadden, A. Al-Zahrani, E. Atenafu, B. Miller, A. Sahgal, C. Menard, N. Laperriere, W. Mason, *J. Neuro. Oncol.* **2013**, *115*, 303–310.
- [15] R. M. Kluck, E. Bossy-Wetzel, D. R. Green, D. D. Newmeyer, *Science* **1997**, *275*, 1132–1136.

Received: September 4, 2015

Revised: November 11, 2015

Published online: December 8, 2015